24th INTERNATIONAL CONGRESS ON SOUND AND VIBRATION
23–27 July 2017, London

PIEZO-RESISTIVE CHARACTERISTICS OF GRAPHENE-BASED CEMENT MATERIALS

Sardar Kashif Ur Rehman, Zainah Ibrahim, Mohammad Faisal Javed and Mohammad Usman Hanif

Department of Civil Engineering, University of Malaya 50603, Kuala Lumpur, Malaysia
email: kashif@engineersdaily.com ; zainah@um.edu.my

Piezo-resistive characteristics of cement-based materials were investigated using graphene nanoplatelets (GNPs). These phenomena provide composite materials with the capability to sense their own strain. In this study, very small amount of GNP (i.e., 0.03% by weight of cement) was used. Results show that compressive strength and strain capability are enhanced by 30% and 80%, respectively, after the addition of GNPs. Electrical resistivity values are decreased by 42% for GNP–cement composite. The fractional change in resistivity confirms that the sensitivity of the GNP–cement composite increases with compressive loading. Therefore, GNP-based cement composites can be an appropriate choice for self-sensing purposes.
Keywords: Cement-based composite; Sensor; Piezo-resistivity; Graphene nanoplatelet; Structural health monitoring

1. Introduction

Monitoring of damage in concrete structures caused by various factors, such as earthquake, wind, ocean waves, or live loads, is important for hazard mitigation. Non-destructive tests offer tools for speedily and effectively monitoring these structures [1]. However, self-sensing concrete that can monitor its own strain is gaining interest from the scientific community. If cement is reinforced with conducting fillers (e.g., carbon materials), then it can observe its own strain by monitoring electrical resistivity values [2]. Self-sensing capability is related to the braking of conducting fibers when cracks initiate in the cement and enhances the resistivity of the overall sample. Resistivity values are closely related to cracks; if cracks open up due to tensile or fracture loading, then resistivity values increase. These values can be decreased through compressive loading. Nanocarbons can fabricate a new kind of high-performance tailored multifunctional cement-based composite that can monitor its real-time damage [3–6]. Carbon nanotubes (CNTs) are composed of sp^2-hybridized carbon atoms as sheets of single-layered graphene rolled up in a cylindrical tube [7]. If these rolled sheets of CNTs open up in one plane, then they form a two-dimensional sheet-like structure. Two-dimensional sheets (e.g., graphene nanoplatelets (GNPs)) exhibit large surface area and high aspect ratio. Sixuan [8] studied the crack depth effect of the GNP-reinforced mortar of cube and prism shapes on the change in electrical resistance and revealed that the cubes and prism specimens respond to the increase in electrical resistance as the crack depth enlarges. The change in electrical resistance for the cube shows a nearly linear trend up to a relative crack depth value of 0.6, and the peak value of the change in electrical resistance is up to 60%. For the prism, only a slight increase in the change in electrical resistance is observed until the relative crack depth value becomes 0.4. Then, the change further increases until peaks at 30% are reached at a relative crack depth value of 0.85. The change in electrical resistance for the cube is more significant than that for the prism at the same relative crack depth. Fu, Ma, Chung, and Anderson [9] used the two-probe method to observe the impedance values in carbon

fiber-reinforced cement mortar. In the two-probe method, two electrical contacts are used to determine the electrical resistance. Wen and Chung [10] determined the damage-sensing characteristics in the longitudinal and transverse directions using the four-probe method. This method involves four electrical contact points; the voltage in the method is measured through the two inner electrical contacts and the current is measured using the two outer electrical contacts. The four-probe method is better than the two-probe method because measured resistance does not include the contact resistance.

Du, Quek, and Dai Pang [11] studied the effect of different concentrations of GNPs on the sensing behavior of cementitious composite and compared it with that for normal cementitious material. They found that using 2.4%–3.6% of GNPs by volume of cement decreases electrical resistivity. As the content of GNPs increases, the fractional change in electrical resistance becomes significant, indicating the increase in piezo-resistivity for the similar strain. The electrical resistance sensitivity to strain is nearly undetectable for GNP content, that is, below the value of 2.4% by volume of cement [11]. Therefore, in this study, we used very small amount (0.03%) by weight of cement of carbon materials as compared with existing research to determine the self-sensing properties of cementitious material. The four-probe method was used for electrical resistance measurement. Strain-sensing and fractional change in resistance were observed and used for determining self-sensing characteristics.

2. Experimental Methodology

2.1 Materials

In this experimental work, the consumed materials were cement, GNP, and superplasticizer. The cement used was Type I Ordinary Portland Cement (Tasek Corporation Berhad), which was the CEM I 42.5 N based on MS EN 197-1. Sika ViscoCrete 2055 (Sika Kimia Sdn. Bhd.) and a third-generation, high-range, and water-reducing polycarboxylate ether-based superplasticizer. Meanwhile, GNP was produced from grade AO-3 GNP Graphene Laboratories, Inc. The properties of GNP are given in Table 1.

Table 1: Properties of GNPs used for the experiment.

Average flake thickness (nm)	12 (30–50 monolayers)
Average particle (lateral) size (nm)	~4500 (1500–10000 nm)
Specific surface area, SSA (m^2/g)	360–400
Purity	99.2%
Color	Black

2.2 Preparation of samples

Cement paste with a water–cement ratio of 0.4 and nanomaterial–cement ratio of 0.03% was used in specimen preparation. One set was labeled as control sample containing pure cement paste, whereas the other set contained GNP. First, dispersion was achieved in deionized water. Then, ultrasonication (Fisher Scientific™ Model 505 Sonic Dismembrator) was performed for 3 min to exfoliate the nanoparticles. The energy that had been introduced into the GNP particles wrecked the interlayer π-bonds. Finally, cement was added to the GNP aqueous solution and mixed thoroughly for 10 min in spar mixer (SP-800A). After the specimen preparation, cement paste was poured into the prism of 160 mm × 40 mm × 40 mm. Thereafter, a stainless-steel wire mesh of 11 mm ×11 mm with an average thickness of 1.3 mm and dimensions of 40 mm × 70 mm was inserted into the samples. The placement of this stainless-steel wire mesh in the specimen is shown in Figure 1(b). The two outer wire meshes

were positioned at 10 mm from the ends of the prism, and the two inner wire meshes were positioned at 40 mm from the outer wire mesh with a length of 60 mm between them.

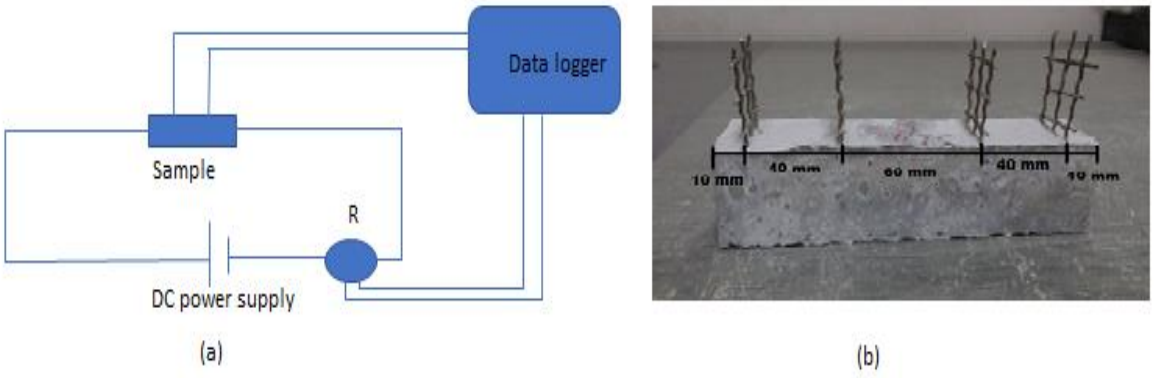

Figure 1: a) Schematic illustration of electric setup and b) position of the wire mesh in the prism-shaped specimen.

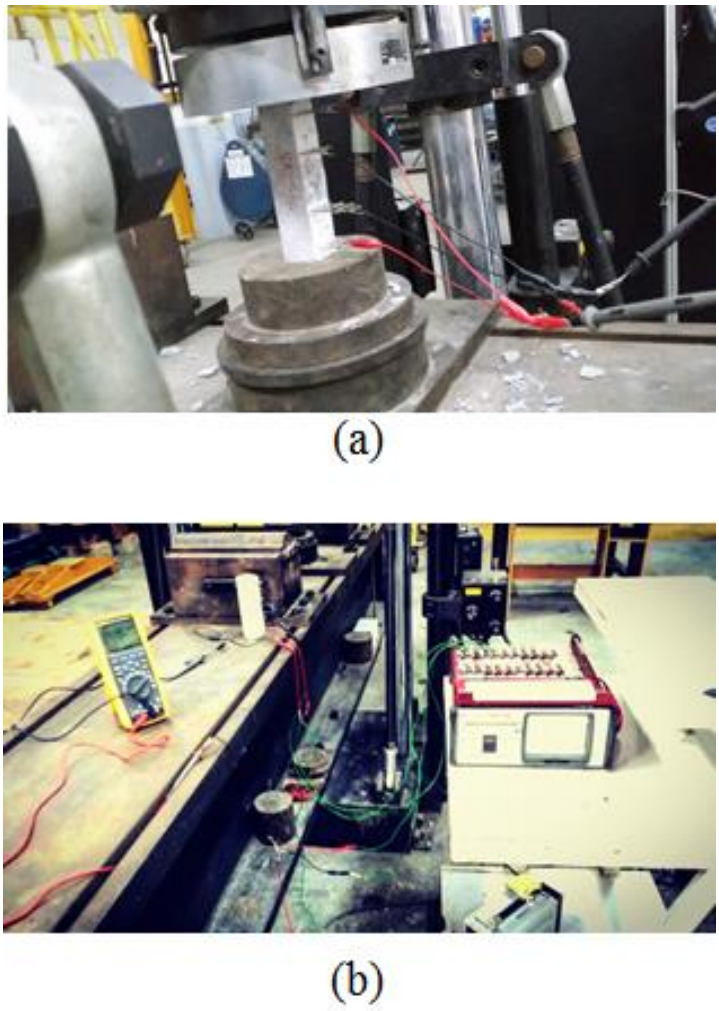

Figure 2: a) Placement of the specimen in the Instron 600 kN machine and (b) Overall setup of the four-probe method for the electrical property testing.

2.3 Test setup for electrical properties

The four-probe method was used to determine the piezo-resistive properties of the specimens. Schematic illustration of the electrical resistivity measurement is shown in Figure 1(a). The method uses the two outer wire meshes to determine the current and two inner wire meshes for the voltage. Experimental investigations were started at the age of 28 days. The setup involves Instron 600 kN machine used for applying a compressive load and TDS-530 data logger to measure the voltage, DC power supply, and 10-ohm resistance. Specimens were placed in the Instron machine, and a constant voltage of 15 V through DC power supply was applied to the samples (Figure 2). 10-ohm resistance was added in series to the electric circuit, and voltage drop was measured across it to determine the electric current in the circuit. Subsequently, the correction factor was used to eliminate the effect of the added 10-ohm resistance to the system. TDS-530 data logger was used to monitor the voltage values. Then, inner wire meshes were connected to the data logger, and the voltage drop was measured in V. One of the outer wire meshes was connected to the negative terminal of the power supply, and another outer wire mesh to the resistor followed by the connection to the second channel of the data logger and positive terminal of the power supply, thereby forming a series circuit.

3. Results

The stress–strain characteristics of the cement paste and GNP-containing cement paste are given in Figure 3. The addition of GNP significantly enhances the load-carrying capacity of the cement paste.

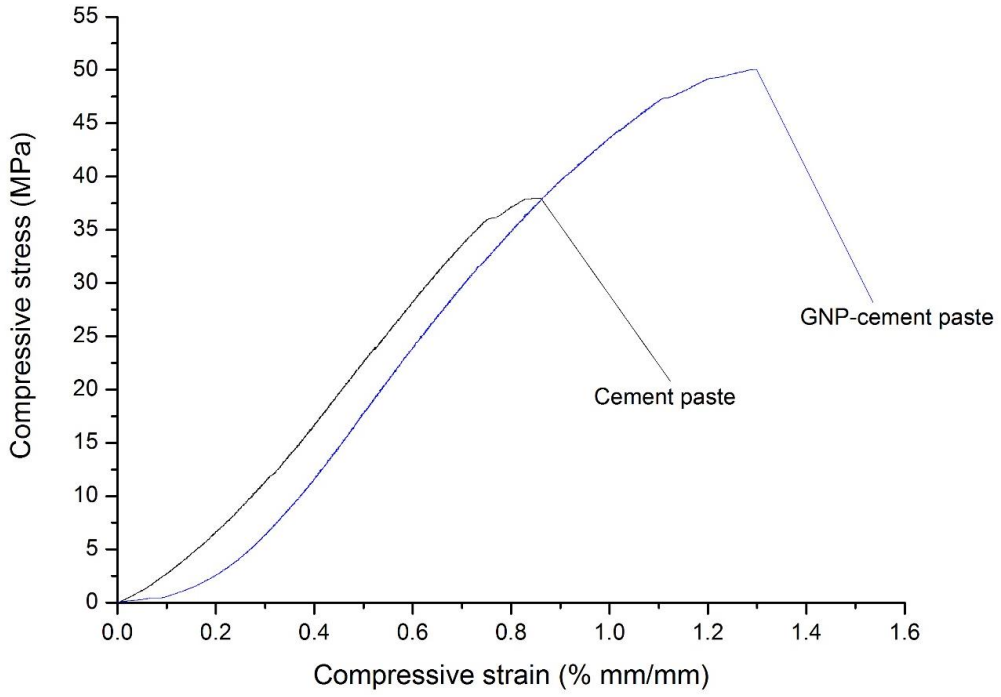

Figure 3: Stress–strain curve for cement paste and GNP–cement paste

Table 2 summarizes the experimental readings for the specimens. Obviously, the addition of the GNP significantly increases the maximum compressive load of cement paste. Electrical resistivity was calculated using the following equation:

$$\rho = \frac{V}{I} * 2\pi * S \quad \text{..... (Equation 1)}$$

where V is the voltage drop in the two inner probes, and I is the current measured by two outer probes. $2\pi S$ is the gematric factor. S is the distance between the probes, and its value (for unequal distance between probes) was calculated from the current carrying probe to the voltage measuring probe.

Table 2: Maximum compressive load and corresponding resistivity values

Specimen	Maximum compressive load (kN)	Four-probe resistivity at maximum compressive loading (kΩ/cm)
Control	61	32.93
GNP–cement paste	80	19.12

Figure 4 illustrates the electrical resistivity values of the samples against the percentage strain. The overall strain capacity is enhanced by 83% in GNP–cement paste sample.

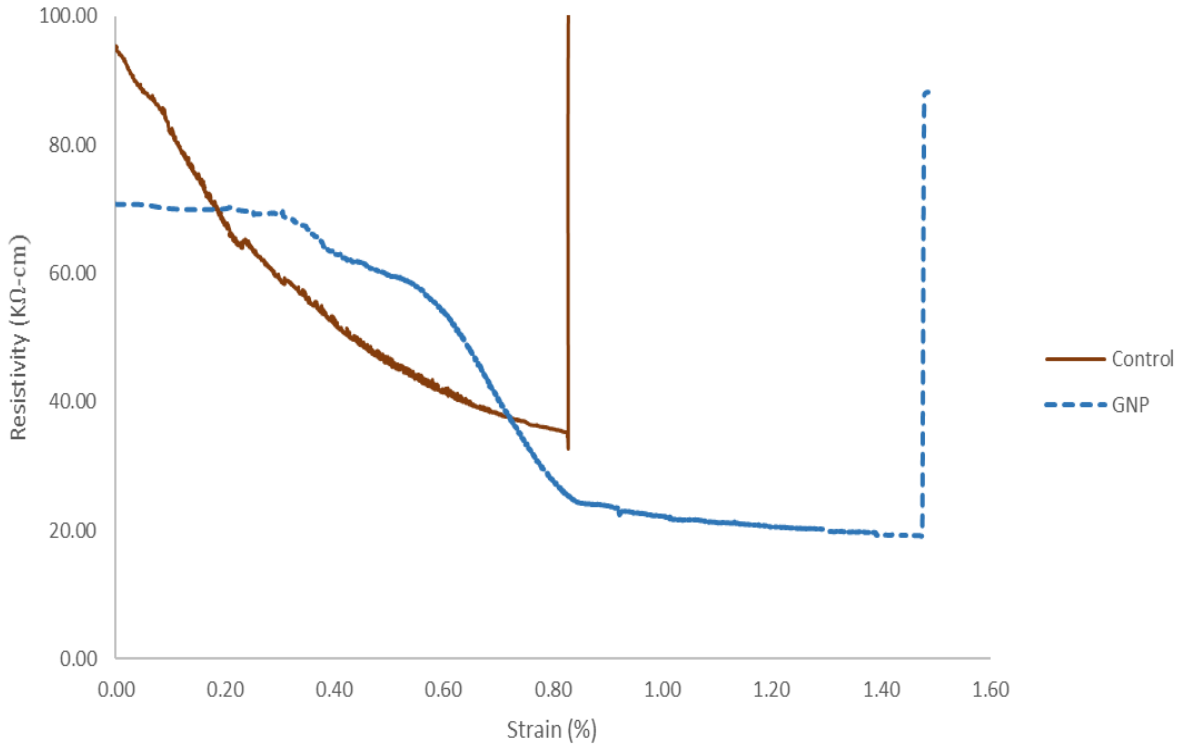

Figure 4: Fractional change in resistance against percentage strain

Normalized compressive loading (NCL) values were calculated to observe the sensing capability of the specimens. NCL is the ratio between the applied load to the maximum compressive load prior to specimen failure. For determining electrical resistance values, the fractional change in resistance (FCR) was used. The selection aimed to achieve simple and convenient comparison of the complex calculated self-sensing values. Equations 2 and 3 present the calculation procedures for the NCL and FCR values.

$$NCL = \frac{P}{P_{max}} \quad \text{..... (Equation 2)}$$

$$FRC = \frac{\rho_t - \rho_o}{\rho_o} \times 100\% \quad \text{..... (Equation 3)}$$

where ρ_t is the electrical resistivity at a given time during the test; ρ_o is the electrical resistivity at the start of the test; P = is the compressive loading at a given time during the test; P_{max} is the maximum compressive loading for the specimen.

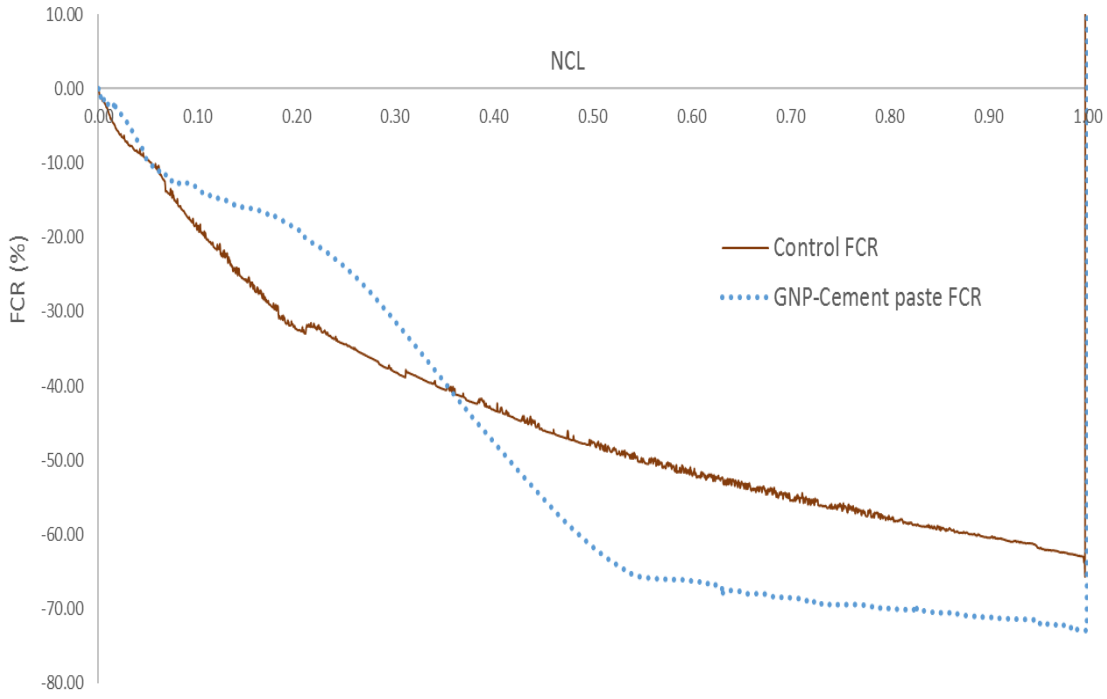

Figure 5: Fractional change in resistance against normalized compression load

4. Discussion

Figure 3 shows that the compressive strength of GNP–cement paste is 30% higher than that of cement paste. Furthermore, the % strain produced in GNP–cement paste is increased up to 83%, indicating its ductile nature. The increases in compressive strength and maximum strain are due to the high graphene strength. In addition, the amount of hydrated products increases with the addition of graphene, thereby resulting in high compressive strength. However, the stiffness of cement paste is higher than that of the GNP–cement paste due to the high GNP ductility.

Electrical resistivity values are reduced by 42% for GNP–cement paste samples. The reduction in the electrical resistivity values of these samples indicates that they possess self-sensing capability.

Figure 4 shows the electrical resistivity values of the control and GNP–cement paste against the strain values. The GNP curve appears straight first and then changes after 0.3%–0.8% of strain loading. The change depicts the formation of cracks and breaking of the GNP particles. However, the curve for the control sample is smooth first and then presents a linear decreasing trend. The reduction in the electrical resistivity values of the control sample is attributed to instrumental error.

Figure 5 represents the fraction change in resistivity values against the normalized compression load. Samples containing GNP have more fractional change in resistance values than the control sample. By increasing the NCL values or compressive loading, the electrical resistance decreases. The curve for the control sample is steep first and then presents a linear trend when load is more than 20%. The occurrence of cracks cannot be accurately predicted by the control sample. Specifically, hairline cracks initiating up until 20% and their propagation cannot be detected by the control sample. In the case of GNP–cement paste, the curve is steep first, then exhibits a sharp decrease in electrical resistance values from 20%–60% of maximum load, and finally presents a linear trend. Therefore, the sensors can accurately sense their own strains when 60%–70% of maximum load is applied. The strain sensing capabilities of these sensors can also be tested using tensile loading.

5. Conclusions

In this study, the piezo-resistive properties of GNP-based cementitious composite were investigated. Electrical resistivity values are decreased by 42% for GNP–cement composite. Compressive strength is increased by 30% and the strain is enhanced by 83% with the addition of 0.03% of GNP. In general, electrical resistance values decrease with the increase in compressive load. When 20%–70% of maximum compressive load is applied, a very steep curve and a rapid decrement are observed. Therefore, these cement composites can act as self-sensing materials and can accurately determine the propagation of cracks.

Acknowledgement

This research was supported by the University Malaya Research Grant (UMRG - Project No. RP004A/13AET), the University Malaya Postgraduate Research Fund (PPP - Project No. PG217–2014B), and the Fundamental Research Grant Scheme, Ministry of Education, Malaysia (FRGS - Project No. FP004-2014B).

REFERENCES

1 Rehman, S. K. U., Ibrahim, Z., Memon, S. A. and Jameel, M. Nondestructive test methods for concrete bridges: A review, *Construction and Building Materials*, **107**, 58-86, (2016).
2 Chung, D. Piezoresistive cement-based materials for strain sensing, *Journal of Intelligent Material Systems and Structures*, **13** (9), 599-609, (2002).
3 Sanchez, F. and Sobolev, K. Nanotechnology in concrete–a review, *Construction and Building Materials*, **24** (11), 2060-2071, (2010).
4 Raki, L., Beaudoin, J., Alizadeh, R., Makar, J. and Sato, T. Cement and concrete nanoscience and nanotechnology, *Materials*, **3**, 918-942, (2010).
5 Sobolev, K. and Gutiérrez, M. F. How nanotechnology can change the concrete world, *American Ceramic Society Bulletin*, **84** (10), 14, (2005).
6 Mukhopadhyay, A. K. Next-generation nano-based concrete construction products: A review. *Nanotechnology in Civil Infrastructure*. Springer, (2011).
7 Vajtai, R. *Springer handbook of nanomaterials*, Springer Science & Business Media, (2013).
8 Sixuan, H., *Multifunctional Graphite Nanoplatelets (GNP) Reinforced Cementitious Composites*, (2012).
9 Fu, X., Ma, E., Chung, D. and Anderson, W. Self-monitoring in carbon fiber reinforced mortar by reactance measurement, *Cement and concrete research*, **27** (6), 845-852, (1997).
10 Wen, S. and Chung, D. Electrical-resistance-based damage self-sensing in carbon fiber reinforced cement, *Carbon*, **45** (4), 710-716, (2007).
11 Du, H., Quek, S. T. and Dai Pang, S. Smart multifunctional cement mortar containing graphite nanoplatelet, *SPIE Smart Structures and Materials+ Nondestructive Evaluation and Health Monitoring*, (2013).